Neuromelanin biosynthesis is driven by excess cytosolic catecholamines not accumulated by synaptic vesicles

David Sulzer*[†‡§], Johanna Bogulavsky*, Kristin E. Larsen*, Gerald Behr*, Erdem Karatekin[¶], Mark H. Kleinman[¶], Nicholas Turro[¶], David Krantz[‖], Robert H. Edwards[‖], Lloyd A. Greene**, and Luigi Zecca[††]

Departments of *Neurology, [†]Psychiatry, **Pathology, and [¶]Chemistry, Columbia University, New York, NY 10032; [‡]Department of Neuroscience, New York State Psychiatric Institute, New York, NY 10032; [‖]Department of Neurology, University of California, San Francisco, CA 94143; and [††]Institute of Advanced Biomedical Technologies, Consiglio Nazionale delle Ricerche, 20090 Segrate, Italy

Contributed by Nicholas Turro, August 25, 2000

Melanin, the pigment in hair, skin, eyes, and feathers, protects external tissue from damage by UV light. In contrast, neuromelanin (NM) is found in deep brain regions, specifically in loci that degenerate in Parkinson's disease. Although this distribution suggests a role for NM in Parkinson's disease neurodegeneration, the biosynthesis and function of NM have eluded characterization because of lack of an experimental system. We induced NM in rat substantia nigra and PC12 cell cultures by exposure to L-dihydroxyphenylalanine, which is rapidly converted to dopamine (DA) in the cytosol. This pigment was identical to human NM as assessed by paramagnetic resonance and was localized in double membrane autophagic vacuoles identical to NM granules of human substantia nigra. NM synthesis was abolished by adenoviral-mediated overexpression of the synaptic vesicle catecholamine transporter VMAT2, which decreases cytosolic DA by increasing vesicular accumulation of neurotransmitter. The NM is in a stable complex with ferric iron, and NM synthesis was inhibited by the iron chelator desferrioxamine, indicating that cytosolic DA and dihydroxyphenylalanine are oxidized by iron-mediated catalysis to membrane-impermeant quinones and semiquinones. NM synthesis thus results from excess cytosolic catecholamines not accumulated into synaptic vesicles. The permanent accumulation of excess catechols, quinones, and catechol adducts into a membrane-impermeant substance trapped in organelles may provide an antioxidant mechanism for catecholamine neurons. However, NM in organelles associated with secretory pathways may interfere with signaling, as it delays stimulated neurite outgrowth in PC12 cells.

Parkinson's disease (PD) results from the death of neuromelanin (NM)-containing neurons in the substantia nigra pars compacta (SNC) (1) and the locus coeruleus (2). The presence of NM provides the characteristic pigmented appearance indicated by the names of these brain regions. NM appears in SNC DAergic neurons within 3 years of birth and increases with age (3). Because the neuronal populations that contain NM are those that die in PD, there has long been speculation that NM underlies PD pathogenesis. In one hypothesis, NM binds neurotoxins such as 1-methyl-4-phenyl-1,2,3,6-tetrahydropyridine (MPTP) (4) or paraquat (5), providing a pool of toxin within pigmented cells. Similarly, NM binds iron and toxic metals that could promote neurodegeneration (6, 7). Finally, NM could itself produce toxic free radicals (8). However, NM cannot be the sole causal factor in PD pathogenesis because all humans accumulate NM with age.

Beyond the suggestions that NM underlies PD, there has been no suggestion of a biological function for this substance. Very little is known about NM biosynthesis, and it is not known where NM is synthesized in the cell, which intracellular or extracellular catecholamine pools are involved, or what triggers its formation (9–12). Although previous studies on NM synthesis have been performed on synthetic polymers arising from spontaneous oxidation in the test tube (13), that substance differs from biological NM (10, 14, 15). In contrast, biological NM is located in subcellular organelles known as NM granules (16). To address long-standing questions on the synthesis, characterization, and functional role of NM granules, we have induced formation of NM in SN neuronal cell culture and a catecholaminergic cell line.

Methods

SNC Cultures. Postnatally derived cultures of ventral midbrain neurons derived from Sprague–Dawley rats were prepared as described (17, 18). Adenovirus constructs were prepared and applied as published (19).

PC12 Cultures. PC12 cells were cultured as described (20). In some cases, we exposed cultures to 50 ng/ml nerve growth factor (NGF; Genentech) to halt cell division and convert them to a neuronal phenotype. Experiments on process outgrowth were performed 5 days postplating and compared cultures derived from the same source culture.
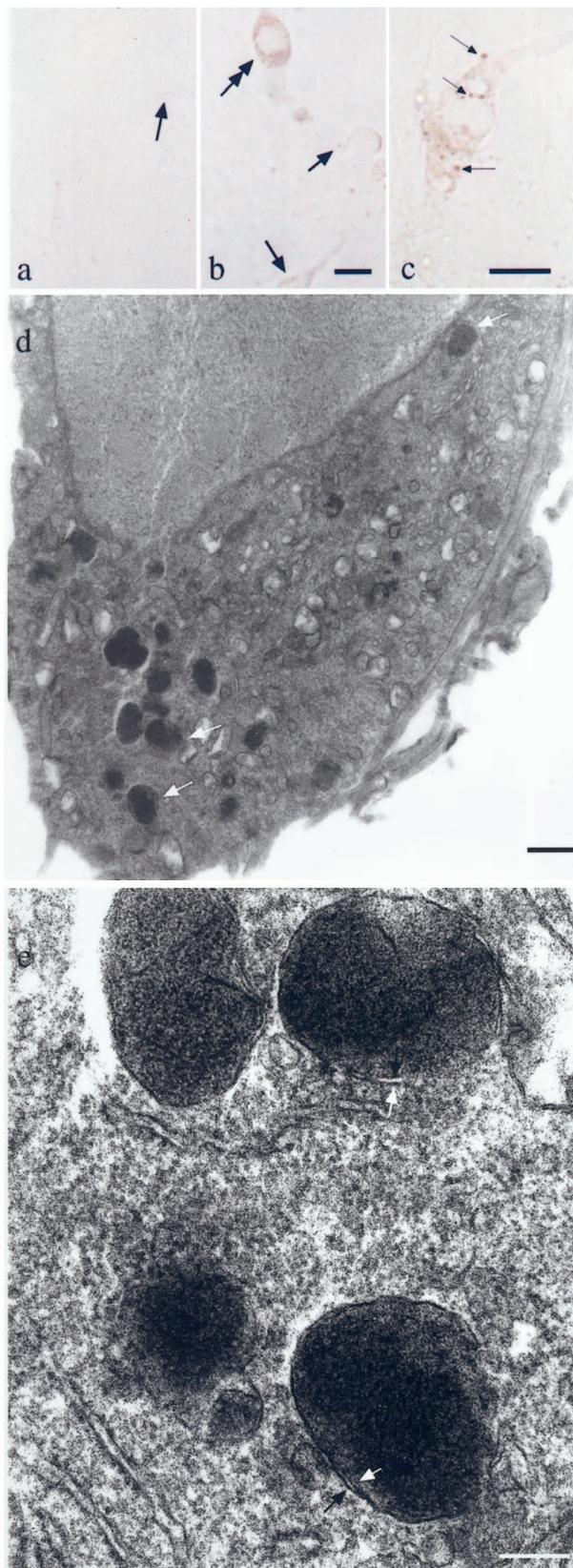
Electron Microscopy (EM). SNC cultures were processed as reported (21). Unpublished micrographs from human brain (seventh decade of life) were generously provided by Virginia Tennyson (Columbia University) and processed as reported (16).

NGF Experiments. PC12 cultures were exposed to 100 μM L- or D-dihydroxyphenylalanine (DOPA) (30 days). At 2- to 3-day intervals, two-thirds of the media were exchanged for media including freshly prepared 100 μM L- or D-DOPA. After 30 days, the cultures were fed twice at 2-day intervals with fresh media without L- or D-DOPA. The cells were replated with two-thirds of the previous medium, and 2.5 ml of freshly prepared medium was added. After 2 days, or 10 days with ongoing media exchange as above, extracellular levels of exogenous DOPA were <300 nM, and cells were exposed to NGF. Cells were scored as exhibiting neurites if ≥1 process extended >1 cell body diameter. For each data point, ≥3 contiguous fields within three separate culture dishes were scored, with ≥100 cells rated per culture. To measure process lengths, digital images of consecutive 10× fields were acquired until ≥30 cell bodies with processes were pictured

NEUROBIOLOGY

CHEMISTRY

Fig. 1. Neuromelanin in cultured neurons. (*a*) Bright-field image of living SNC neurons exposed to vehicle and photographed 3 weeks postplating. In these control cultures, no pigment was observed. Arrows indicate examples of cell bodies. (*b*) Bright-field image of living SNC neurons derived from the same dissection exposed to 50 μM L-DOPA (11 days). Dark brown NM granules are distributed in a pattern identical to that in SNC neurons in human brain. The

granule distribution was primarily in cell bodies. The double-headed arrow indicates the most highly NM-expressing cell in the field. Less pigmented cells are indicated with single-headed arrows. (Scale bar = 5 μm.) (*c*) A higher-magnification bright-field image of NM in living SNC culture after exposure to 50 μM L-DOPA (14 days). Arrows indicate samples of NM granules that are in focus in this plane. (Scale bar = 5 μm.) (*d*) NM granules in a cultured SN neuron exposed to 50 μM L-DOPA (14 days). The white arrows indicate individual NM granules. The granules are essentially identical to those in human SN, although there is little or no lipofuscin. Sections are stained with osmium and uranyl acetate only. (Scale bar = 1 μm.) Controls do not display NM. (*e*) At higher power, a double membrane is discerned (arrows) as in NM granules *in vivo*. (Scale bar = 200 nm.)

from four cultures per category (i.e., >120 cells per category). When a neurite branched, the longer of the branches was traced. Neurite length is reported as the mean process length normalized for the number of cell bodies in the fields.

NM Isolation. Detailed methods are available on the web at http://www.columbia.edu/~ds43/EPR.html. In short, to isolate NM, frozen cells were frozen and thawed, pelleted, incubated to 5 mg/ml SDS, sonicated, pelleted, resuspended in proteinase K (Sigma), pelleted, resuspended in methanol, resuspended in hexane, pelleted, and dried under N_2 gas.

Electron Paramagnetic Resonance (EPR) Techniques. Detailed methods are available on the web at http://www.columbia.edu/~ds43/EPR.html. In short, samples were placed into a suprasil quartz dewar filled with liquid N_2 and measured by using a Bruker ESP380E and Bruker EMX EPR spectrometer operating at 9–10 GHz. Spectra were taken at 77 K and 100-KHz modulation amplitude. EPR data are expressed as the first derivative of the absorption related to the increase in applied magnetic field.
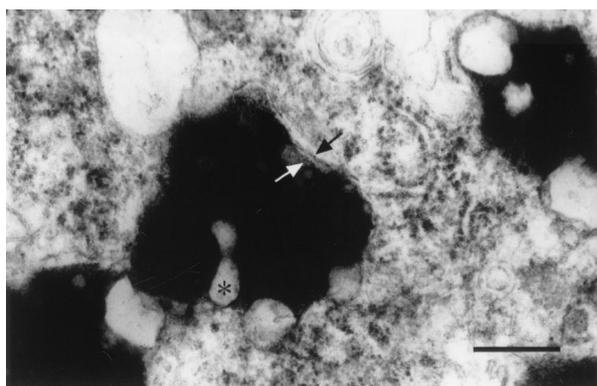
Results

Induction of Substantia Nigra (SN) NM by L-DOPA. As dopamine (DA) forms a dark pigment after oxidation to a quinone, it has been suggested that DA could be the precursor to NM (13). Addition of DA to the medium induced degeneration in SNC cultures (not shown), as reported (22). In contrast, the DA precursor L-DOPA at concentrations of 50–100 μM is neurotrophic in SNC cultures at up to 5 days of exposure (18). L-DOPA is rapidly converted to DA in the cytosol as quantal size is increased $\approx$4-fold in 30 min by L-DOPA (50 μM) (23). We therefore hypothesized that L-DOPA might produce NM with longer exposure.

We exposed postnatal rat-derived ventral midbrain cultures to 50 μM L-DOPA twice, on days 5 and 12 *in vitro*. By 11–14 days, deep brown granules in a typical NM distribution were clearly visible by light microscopy in living neurons (Fig. 1 *a–c*). The granules were prominent in the cell body, negligible in processes, and excluded from nuclei. Therefore, whereas rat SN neurons do not normally contain noticeable NM, they can be induced to form NM. Neurons that expressed NM possessed a very electron dense precipitate that filled membrane-bound organelles (Fig. 1 *d* and *e*). These were 200–1,000 nm in diameter, possessed double membranes separated by $\approx$15 nm, and were essentially identical to human NM granules observed by EM (Fig. 2). Lipofuscin, which is present in older human NM granules from the third decade, is absent in cultured NM granules. NM granules do not occur in untreated cultures and to our knowledge have not been previously reported in neuronal culture.

To estimate the quantity of NM induced by L-DOPA, we counted pigmented granules visible in neuronal cytoplasm under bright-field microscopy (Fig. 3*a*). By 26 days of exposure, L-DOPA induced >10 pigmented granules in > 95% of the

Fig. 2. Human NM granules. NM granules from human SN. The arrows indicate the double membranes. ∗ indicates lipofuscin deposits within the granules. (Scale bar = 100 nm.)

neurons, whereas in control cultures >90% of the neurons lacked any pigmented granules. The antioxidant l-*n*-acetylcysteine (L-NAC) at an exposure that decreases extracellular quinones induced by L-DOPA in the ventral midbrain cultures (24) did not block formation of L-DOPA-induced pigmented granules.

Adenoviral vector-mediated overexpression of the brain vesicular monoamine transporter (VMAT2) in ventral midbrain DA cultures increased the number of DA molecules released by synaptic vesicles ≈4-fold because of increased sequestration (19). VMAT2 does not mediate DOPA accumulation (25), and VMAT2 does not induce DOPA accumulation into cell lines (Doris Peter and R.E., unpublished work).

To examine the role for cytosolic DA in NM synthesis, we infected SNC cultures with the viral vector. Approximately 90% of the neurons express the recombinant VMAT2 (19). However, degeneration of astrocytes was noted beginning at 10 days of exposure to virus and so we used a shorter duration of DOPA exposure (50 μM L-DOPA for 7 days) than in Fig. 3*a*. Although this exposure induced less NM expression, pigment was clearly visible. VMAT2-overexpressing cultures showed reduced expression of NM in comparison to similarly exposed noninfected cultures (Fig. 3*b*). These findings are consistent with the interpretation that cytoplasmic DA drives formation of NM.

The association of Fe^{3+} radical with NM observed with EPR (see below) suggested a role for Fe^{3+} in NM synthesis. The effect of increased Fe^{3+} could not be determined in SNC cultures because the midbrain DA neuronal cultures are killed by low levels of exogenous Fe^{3+} (not shown). Therefore, we exposed neuronal cultures to the iron chelator desferrioxamine (DES), which would be expected to bind iron already present in the culture. DES (10 μM) or vehicle was added to the cultures 18 h before adding L-DOPA (50 μM, 7 days). DES inhibited NM induction by L-DOPA nearly to control levels (Fig. 3*b*). We conclude that iron participates in NM synthesis.

NM Induction by D-DOPA. D-DOPA is not normally converted to DA and is severely neurotoxic in SN culture (18). We therefore exposed PC12 cells, a DAergic pheochromocytoma cell line, to 100 μM L- or D-DOPA for 14 days to 3 months. During these exposures the cells undergo cell division at normal rates (not shown). Therefore, PC12 cells are resistant to D-DOPA neurotoxicity.

L-DOPA is detectably converted to DA in PC12 cell cultures in <90 s (26). In preliminary studies, we found that 24 h after 100 μM D-DOPA, there was no increase in either catecholamine release or total cellular catecholamine (not shown). Therefore, D-DOPA is not metabolized to DA in PC12 cells.
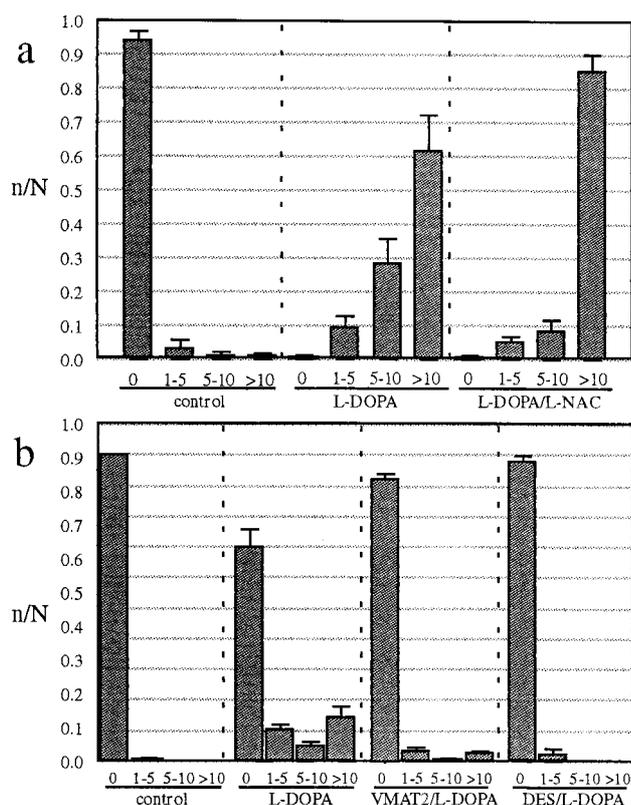
Fig. 3. (*a*) Expression of NM granules. Granules were counted in SN cultures and scored as displaying 0, 1–5, 5–10, or >10 pigmented granules per neuron (mean ± SEM, four culture dishes per condition, = 100 cells rated per culture dish). The cultures were derived from the same batch of SNC dissections and were exposed to vehicle, L-DOPA, or L-DOPA with L-NAC once, and fixed (so that the age would be identical for all groups) 26 days after exposure. The data are displayed as fraction of neurons within each category (i.e., *n* of neurons in a bin of #granules/*N* of total neurons in that treatment). There was an increase in pigmented granules for L-DOPA (50 μM) over controls ($P < 0.001$, χ^2 test) and L-DOPA with L-NAC (500 μM) over controls ($P < 0.001$, χ^2 test). The total number of surviving neurons was not different between the three conditions. L-NAC-only treated cultures showed no pigmented granules. (*b*) Effect of VMAT2 overexpression and DES. Cultures derived from the same batch of SNC dissections were induced to overexpress VMAT2 by exposure to an adenoviral vector. Control cultures were exposed to a similar adenovirus construct that lacked the VMAT2 sequence. Cultures then were exposed to vehicle or L-DOPA and fixed 7 days after exposure. There was an increase in pigmented granules for L-DOPA (50 μM) over controls ($P < 0.001$, χ^2 test). VMAT2 overexpressing cultures exposed to L-DOPA displayed fewer pigmented granules than L-DOPA alone ($P < 0.001$, χ^2 test in both this trial and an independent experiment where cultures were exposed to L-DOPA for 14 days). Cultures that overexpressed VMAT2 but were not exposed to L-DOPA showed no pigmented granules (not shown). Cells exposed to both L-DOPA and DES (10 μM) displayed fewer pigmented granules than L-DOPA alone ($P < 0.001$, χ^2 test in two separate trials). DES-only treated cultures showed no pigmented granules (not shown).

Both L-DOPA and D-DOPA-induced brown granules were observed with light microscopy in PC12 cells after long-term exposure (>2 months), although less prominently than in SNC neurons (not shown). Pigment was never observed in controls. NM granules could be clearly differentiated from large dense core granules that normally accumulate catecholamines in PC12 cells (Fig. 4). Large dense core granules had diameters of ≈150 nm and single membranes. In contrast, NM granules were ≈500 nm in diameter and had double membranes. Under light microscopy we observed no incorporation of exogenous synthetic "NM" produced by autoxidation of 10 mM D-DOPA into cells
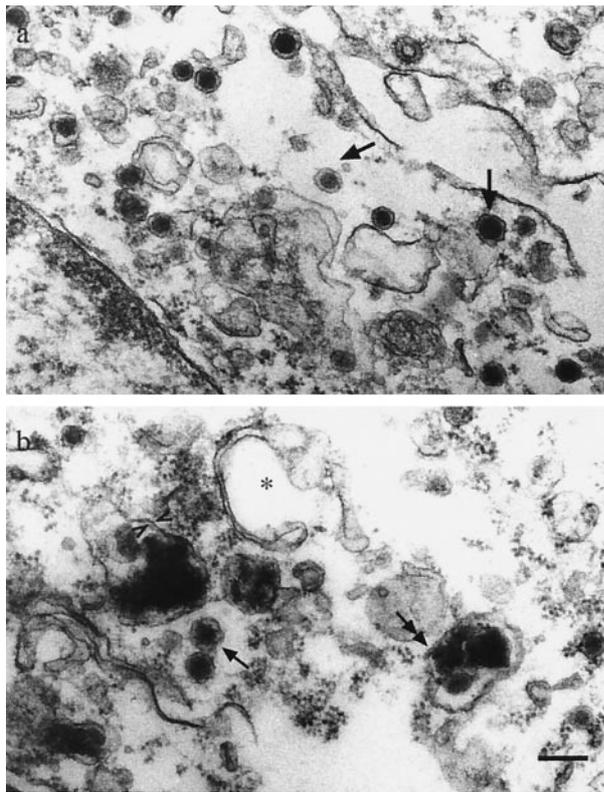
Fig. 4. NM in PC12 cells. (*a*) In control PC12 cells, the small electron dense bodies (single-headed arrows) are normal secretory dense core granules. (*b*) In cultures exposed to 100 μM D-DOPA for 60 days (NGF added on day 50), both dense core granules (single-headed arrows) and larger NM granules (double-headed arrows) are observed. A double membrane is indicated by arrowheads. * indicates a classic autophagic vacuole. (Scale bar = 200 nm.)

by 2 weeks of exposure (not shown). Therefore, NM appears to be synthesized within cells rather than taken up (27).

Identification of NM by EPR. The classical Schmorl method (28) produced a diffuse reaction product in cell bodies of D-DOPA-treated PC12 cells indicative of NM (not shown). The most widely practiced contemporary approach for NM identification is EPR, which yields characteristic resonant frequencies for different organic and inorganic radicals (7, 29). We used PC12 cultures for EPR, as we realized that it would be difficult to obtain sufficient quantities of NM in SNC cultures, because of the low number of neurons per postnatal mouse.

In human NM there are two EPR peaks, one at a characteristic frequency for π-electron semiquinone free radical (3,400 G; a $g = 2$ peak), and the other to bound Fe^{3+} in a high spin configuration (1,600 G; a $g = 4$ peak) (10, 29). PC12 cells displayed both peaks (Fig. 5a). Additional less-defined peaks were sometimes observed close to the semiquinone, likely because of metal binding. Ethylenediaminetetraacetic acid (150 mM for 8 h) removed the iron radical peak by chelating ferric iron and dissociating it from NM.

Although EPR is accurate for measuring unpaired electrons, NM is underestimated in these measurements because of electron trapping by nearby compounds and more complete oxidation of the semiquinone to the nonradical quinone. D-DOPA-treated (100 μM, 2–3 months, no NGF) cultures always showed higher amplitudes of semiquinone peaks than control cultures (28–50% increased amplitude of $g = 2$ peak, in five separate experiments; Fig. 5b). L-DOPA-treated cultures gave variable
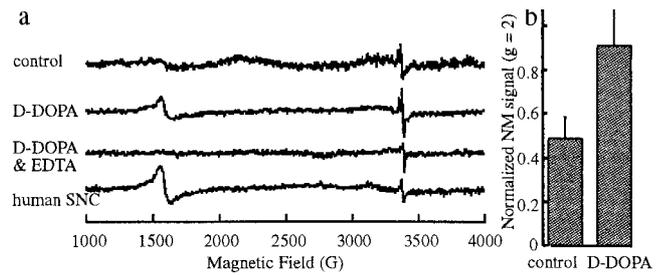

Fig. 5. EPR of cell culture and human NM. (*a*) EPR spectra of control PC12 cells exposed to vehicle for 3 months; PC12 cells derived from the same parent culture exposed to 100 μM D-DOPA for 3 months; isolated NM from PC12 cells after EDTA treatment, which removes the peak corresponding to iron radical; and isolated NM from human SNC. The two peaks in human NM are at identical positions to the major peaks in PC12 cells. (*b*) Amplitudes of the semiquinone peaks for the control PC12 cultures and the cultures exposed to D-DOPA. The bars indicate the mean amplitude ± SEM (three readings) from cells derived from the same parent culture.

peak heights at identical resonant frequencies to D-DOPA cultures and human NM (not shown).

Effects on Growth Factor Response. PC12 cells extend neurites after exposure to NGF (30). We found that promotion of neurite outgrowth by NGF in D-DOPA treated NM-expressing PC12 cell cultures was delayed by about 5 days ($P < 0.001$, Komolgorov Smirnov test, $\lambda = 2.29$; Fig. 6; similar results observed in five independent trials). The delayed response occurred both in cultures where DOPA was diluted out over 6 days and 12 days before NGF exposure with final maximum levels of 300 and 3 nM, respectively (see *Methods*). L-DOPA-treated NM-expressing PC12 cell cultures showed similar results (not shown). To confirm that neurites were shorter, we fixed the cultures and measured process lengths. At 2 days post-NGF, D-DOPA decreased process length (for the relatively infrequent process that were expressed) by 60% from control values ($P < 0.01$, t test, $F = 1.36$; similar results observed in three separate trials).

Discussion

NM is found in deep brain structures within neuronal populations that degenerate in PD and so it has been suggested to
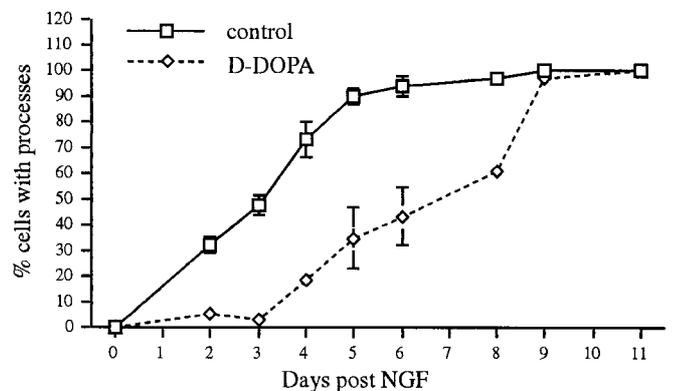
Fig. 6. Conditions that promote NM synthesis delay neurite outgrowth. Cells were scored as displaying processes if they exhibited a neurite that extended at least one cell body length. Cells were exposed to 100 μM D-DOPA for 30 days, with replacement of medium containing the compound in 2- to 3-day intervals. After two additional replacements with medium without D-DOPA and subsequent washing, NGF (50 mg/ml) was added. The cells were scored at 1- to 2-day intervals for neurite outgrowth ($n = 3$ cultures, 100 cells scored per culture, ± SEM). Similar results were observed in five independent experiments and after similar L-DOPA exposure (not shown).
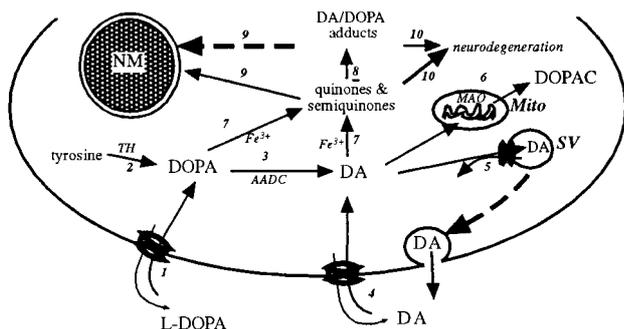
Fig. 7. Proposed model for NM synthesis in SN DA neurons. 1) L-DOPA is taken up by a plasma membrane amino acid transporter. 2) L-DOPA is synthesized endogenously by tyrosine hydroxylase (TH). 3) DA is produced by aromatic acid decarboxylase (AADC). 4) Additional cytosolic DA is by the DA uptake transporter. 5) Synaptic vesicles (SV) and endosomes (not shown) accumulate cytosolic DA via VMAT2. 6) Cytosolic DA is metabolized in mitochondria (Mito) via monoamine oxidase. 7) Excess cytosolic DA and DOPA is oxidized via iron catalysis to quinones and semiquinones in the cytosol. 8) Quinones react with cysteine, proteins, and lipids. 9) DA-derived quinones and DA adducts in the cytosol and organelles are phagocytosed in bilamellar autophagic vacuoles/lysosomes where they are permanently stored as NM. 10) Damage from quinone-derived adducts that are not accumulated in NM granules promote neurodegeneration.

mediate this neurodegeneration. However, study of NM has been limited to chemical analysis of human NM derived from autopsy. In this study, we induced NM in neuronal culture to address controversies on the synthesis and function of this substance. We find: (*i*) NM is derived from cytosolic DA and DOPA quinone and their oxidized metabolites, (*ii*) NM synthesis is inhibited by VMAT2 overexpression, (*iii*) NM synthesis is catalyzed by Fe^{3+} (in contrast to tyrosinase), and (*iv*) NM interferes with NGF response. The results suggest that, rather than promoting neurodegeneration, NM may provide an antioxidant mechanism by irreversibly sequestering reactive catecholamine metabolites within an organelle removed from the cytosol.

Identification of NM in Culture. Although rodent SNC neurons have very low NM (31) this is apparently not an inherent property. The deep brown electron dense granules in cultured SNC neurons or PC12 cells are identified as containing NM by several criteria: (*i*) the distribution, which is punctate, high in the cell body, negligible in processes, and excluded from the nucleus, is typical for SNC NM; (*ii*) the deep brown pigment in living and fixed SNC neurons at the light level is identical to human NM; (*iii*) ultrastructurally, the double membrane organelles in SNC neurons and PC12 cells are identical to human brain NM granules; (*iv*) the electron dense substance within these organelles appears identical to NM in younger human SNC; (*v*) EPR indicates an identical organic radical peak for human SNC and PC12 cell NM; and (*vi*) cultured and human NM display the identical interaction with Fe^{3+} radical.

Models for NM Synthesis. The level of cytosolic catechols is maintained by feedback inhibition of tyrosine hydroxylase, mitochondrial monoamine oxidase, and VMAT2-mediated accumulation into synaptic vesicles and associated structures. If the level of cytosolic DA is not well regulated, DA-derived cytosolic quinones and semiquinones could react with proteins, lipids, and nucleic acids (32). We suggest NM biosynthesis acts as an additional mechanism for regulating cytosolic DA and DA quinone levels by sequestering these products and their adducts in autophagic vacuoles (Fig. 7).

Both L-DOPA, which is rapidly converted to DA in the cytosol of cells that possess DOPA decarboxylase, and D-DOPA, which is not converted to DA in our systems, induce NM. DOPA uptake occurs via a widely expressed cation amino acid transporter (33). In SNC cultures the fraction of DAergic neurons is 10–40% with the remainder mostly GABAergic, but more than 90% of the neurons display NM with sufficient DOPA exposure. Therefore, NM synthesis does not depend on the conversion of DOPA to DA, and both DA and DOPA can act as NM precursors.

Our findings indicate that NM and eumelanin synthesis differ in important ways. Eumelanins are synthesized from tyrosine via tyrosinase to DOPA-quinone within the melanosome lumen (34). In melanocytes, melanosomes are specialized lysosomes enclosed by single membranes (35). In contrast, NM apparently is synthesized by accumulation of cytosolic DA and DOPA derivatives formed in the cytosol via iron catalysis and trafficked into double membrane autophagic organelles. Extracellular NM does not appear to be accumulated.

The double membrane of both the DOPA-induced and human NM granule indicates that these are autophagic vacuoles. Except for the presence of very dark pigment, the organelles are morphologically identical to lipofuscin granules (Fred Dice, personal communication). Normally, autophagic vacuoles occur during fasting and fuse with tertiary lysosomes within ≈10 min. In contrast, lipofuscin granules are arrested in fusion and may last throughout the cell's lifetime (36). NM granules display the lysosomal marker acid phosphatase (37) and thus share characteristics with classical lysosomes. More importantly, NM granules are >1,000-fold greater in volume than a synaptic vesicle and would provide a massive sink for cytosolic DA.

DA-derived NM (via L-DOPA), synthesis is inhibited by overexpression of VMAT2. Because VMAT2 decreases cytosolic DA by increasing synaptic vesicle DA sequestration (19), the results suggest that NM is induced by high cytosolic DA. The finding that ventral tegmental DA neurons express VMAT2 at significantly higher levels than SNC (38) may contribute to the previously unexplained observation that DAergic SNC neurons display far more NM than neighboring DAergic ventral tegmental area neurons.

The antioxidant L-NAC decreases extracellular quinones induced by L-DOPA in ventral midbrain cultures (24) but did not block formation of L-DOPA-induced NM. Although cysteinyl-DA has been suggested to inhibit NM formation (39), our findings suggest that NM can be formed from intracellular cysteinyl-DA, analogous to formation of pheomelanin, the pigment in red hair (28). Indeed, analysis of autopsy material suggests cysteinyl-DA as a component of SNC NM (40).

Fe^{3+} and NM Formation. Conversion of DA to NM is promoted by iron because the chelator DES blocks NM synthesis. This finding appears to answer a long-standing question by showing that iron catalyzes NM synthesis (10). The EPR results suggest that iron not only promotes NM synthesis but continues to bind to NM. We did not observe tyrosinase immunoreactivity in SN cultures (not shown). Although these results support Fe^{3+}-mediated catalysis of DOPA and DA to NM, an alternate mechanism could be by inhibition of an enzyme that requires an iron cofactor, and several catalytic processes for DA oxidation have been proposed (reviewed in ref. 32).

Effect of NM on NGF-Induced Neurite Outgrowth. The endosomal/lysosomal pathway participates in membrane transport and recycling of cell surface receptors and receptor ligands. For example, NGF promotes neurite outgrowth in PC12 cells (30) after binding to the trkA receptor. The NGF/trkA complex is delivered into endosomes that undergo retrograde transport and participate in activation of neurite outgrowth (41). Exposure to

DOPA (50–200 μM for 1–4 days) potentiates, rather than inhibits, NGF-stimulated neurite outgrowth in PC12 cells (24). However, in cells with DOPA exposure sufficient to induce NM formation, this response to NGF was significantly delayed. This was not because of an acute sublethal toxic effect of DOPA *per se*, because exogenous DOPA was withdrawn long before NGF exposure. Therefore, the lag in neurite outgrowth after NGF exposure appears to be related to a long-lasting effect of DOPA itself, such as NM formation. It may be that NM in lysosome-associated organelles interferes with trafficking in growth factor pathways, similar to results with lipofuscin granules (42).

Models of NM Effects. NM synthesis could provide a novel antioxidant mechanism by trapping cytosolic quinones and semiquinones in lysosome-associated organelles so that they are no longer reactive with cytosolic components. These reactive metabolites, which remain in part in a free radical state as shown by EPR, are permanently sequestered in these organelles as they are converted to an insoluble compound that cannot diffuse back to the cytosol, thus protecting SNC cytosol from accumulating damage over many years. In analogy, some antioxidants work by sequestering oxyradicals, e.g., vitamin E sequesters oxyradicals by reaction with its chromanol moiety, and eumelanin sequesters UV light-induced radicals.

Thus, rather than playing a role in neuronal death associated with PD, NM may be a marker for neurons that display excessive free cytosolic catecholamines. A neuroprotective property of NM biosynthesis would be consistent with the previously puzzling observation that although NM neurons degenerate in PD, some highly NM-expressing cells survive in advanced stages of the disease (43). Humans may normally experience catecholamine-mediated oxidative stress in the cytosol of SN and locus coeruleus neurons, but NM synthesis together with other antioxidant mechanisms may be sufficient to maintain neuronal viability, except in the case of PD. However, although NM synthesis may be neuroprotective, its long-term accumulation may have deleterious consequences. For example, an NM-mediated disruption of receptor-ligand trafficking or lysosomal/secretory organelle function could explain the effects of long-term DOPA exposure on NGF-promoted neurogenesis.

1. Kastner, A., Hirsch, E. C., Lejeune, O., Javoy-Agid, F., Rascol, O. & Agid, Y. (1992) *J. Neurochem.* **59,** 1080–1089.
2. Bertrand, E., Lechowicz, W., Szpak, G. M. & Dymecki, J. (1997) *Folia Neuropathol.* **35,** 80–86.
3. Foley, J. M. & Baxter, D. (1958) *J. Neuropathol. Exp. Neurol.* **7,** 586–598.
4. D'Amato, R. J., Alexander, G. M., Schwartzman, R. J., Kitt, C. A., Price, D. L. & Snyder, S. H. (1987) *Life Sci.* **40,** 705–712.
5. Lindquist, N. G., Larsson, B. S. & Lydén-Sokolowski, A. (1988) *Neurosci. Lett.* **93,** 1–6.
6. Zecca, L., Pietra, R., Goj, C., Mecacci, C., Radice, D. & Sabbioni, E. (1994) *J. Neurochem.* **62,** 1097–1101.
7. Shima, T., Sarna, T., Swartz, H. M., Stroppolo, A., Gerbasi, R. & Zecca, L. (1997) *Free Radical Biol. Med.* **23,** 110–119.
8. Enochs, W. S., Sarna, T., Zecca, L., Riley, P. A. & Swartz, H. M. (1994) *J. Neural. Transm. Parkinson's Dis. Dementia Sect.* **7,** 83–100.
9. Miranda, M., Botti, D. & Di Cola, M. (1984) *Mol. Gen. Genet.* **193,** 395–399.
10. Zecca, L., Shima, T., Stroppolo, A., Goj, C., Battiston, G. A., Gerbasi, R., Sarna, T. & Swartz, H. M. (1996) *Neuroscience* **73,** 407–415.
11. Xu, Y., Stokes, A. H., Freeman, W. M., Kumer, S. C., Vogt, B. A. & Vrana, K. E. (1997) *Mol. Brain Res.* **45,** 159–162.
12. Tief, K., Schmidt, A. & Beerman, F. (1998) *Mol. Brain Res.* **53,** 307–310.
13. Graham, D. G. (1978) *Mol. Pharmacol.* **14,** 633–643.
14. Zecca, L., Costi, P., Mecacci, C., Ito, S., Terreni, T. & Sonnino, S. (2000) *J. Neurochem.* **74,** 1758–1765.
15. Zareba, M., Bober, A., Korytowski, W., Zecca, L. & Sarna, T. (1995) *Biochim. Biophys. Acta* **1271,** 343–348.
16. Duffy, P. E. & Tennyson, V. M. (1965) *J. Neuropathol. Exp. Neurol.* **24,** 398–414.
17. Rayport, S., Sulzer, D., Shi, W. X., Sawasdikosol, S., Monaco, J., Batson, D. & Rajendran, G. (1992) *J. Neurosci.* **12,** 4264–4280.
18. Mena, M. A., Davila, V. & Sulzer, D. (1997) *J. Neurochem.* **69,** 1398–1408.
19. Pothos, E. N., Larsen, K. E., Krantz, D. E., Liu, Y.-J., Edwards, R. H. & Sulzer, D. (2000) *J. Neurosci.* **20,** 7297–7306.
20. Yan, C. Y. I. & Greene, L. A. (1998) *J. Neurosci.* **18,** 4042–4049.
21. Sulzer, D. & Rayport, S. (1990) *Neuron* **5,** 797–808.
22. Rosenberg, P. A. (1988) *J. Neurosci.* **8,** 2887–2894.
23. Pothos, E., Davila, V. & Sulzer, D. (1998) *J. Neurosci.* **18,** 4106–4118.
24. Mena, M. A., Davila, V., Bogaluvsky, J. & Sulzer, D. (1998) *Mol. Pharmacol.* **54,** 678–686.
25. Slotkin, T. A. & Kirshner, N. (1971) *Mol. Pharmacol.* **7,** 581–592.
26. Pothos, E. N., Desmond, M. & Sulzer, D. (1996) *J. Neurochem.* **66,** 629–636.
27. Offen, D., Gorodin, S., Melamed, E., Hanania, J. & Malik, Z. (1999) *Neurosci. Lett.* **260,** 101–104.
28. Pearse, A. G. E. (1985) *Histochemistry: Theoretical and Applied* (Churchill Livingstone, Edinburgh).
29. Sarna, T., Hyde, J. S. & Swartz, H. M. (1976) *Science* **192,** 1132–1134.
30. Tischler, A. S. & Greene, L. A. (1978) *Lab. Invest.* **39,** 77–89.
31. DeMattei, M., Levi, A. C. & Fariello, R. G. (1986) *Neurosci. Lett.* **72,** 37–42.
32. Sulzer, D. & Zecca, L. (2000) *Neurotoxicity Res.* **1,** 181–195.
33. Gomes, P., Serrao, M. P., Viera-Coelho, M. A. & Soares-da-Silva, P. (1997) *Cell Biol. Int.* **21,** 249–255.
34. Calvo, P. A., Frank, D. W., Bieler, B. M., Berson, J. F. & Marks, M. S. (1999) *J. Biol. Chem.* **274,** 12780–12789.
35. Schraermeyer, U., Peters, S., Thumann, G., Kociok, N. & Heimann, K. (1999) *Exp. Eye Res.* **68,** 237–245.
36. Terman, A. & Brunk, U. T. (1998) *Mech. Ageing Dev.* **104,** 277–291.
37. Barden, H. (1970) *J. Neuropathol. Exp. Neurol.* **29,** 225–240.
38. Nirenberg, M. J., Chan, J., Liu, Y., Edwards, R. H. & Pickel, V. M. (1996) *J. Neurosci.* **16,** 4135–4145.
39. Li, H., Shen, X. M. & Dryhurst, G. (1998) *J. Neurochem.* **71,** 2049–2062.
40. Zecca, L., Parati, E., Mecacci, C. & Seraglia, R. (1992) *Biochim. Biophys. Acta* **1138,** 6–10.
41. Grimes, M. L., Zhou, J., Beattie, E. C., Yuen, E. C., Hall, D. E., Valletta, J. S., Topp, K. S., LaVail, J. H., Bunnett, N. W. & Mobley, W. C. (1996) *J. Neurosci.* **16,** 7950–7964.
42. Terman, A., Dalen, H. & Brunk, U. T. (1999) *Exp. Gerontol.* **34,** 943–957.
43. Gibb, W. R. G. (1992) *Brain Res.* **581,** 283–291.